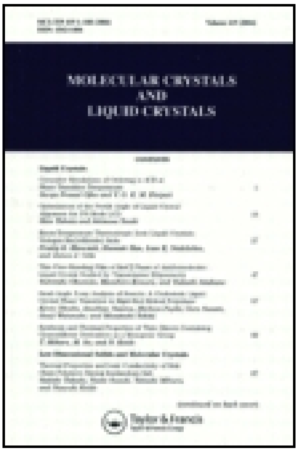

Molecular Crystals and Liquid Crystals
Publication details, including instructions for authors and subscription information:
http://www.tandfonline.com/loi/gmcl20

Chemically Crosslinked Copolymer Electrolytes Based on Imidazole for Quasi-Solid State Dye-Sensitized Solar Cells

Young-Keun Kim [a], Sang-Eun Cho [a], Won-Pill Hwang [a], Min-Hye Seo [a], Hyun-Woo Park [a], Mi-Ra Kim [a] & Jin-Kook Lee [a]

[a] Department of Polymer Science & Engineering, Pusan National University, Jangjeon-dong, Kuemjeong-gu, Busan, 609-735, Korea

Version of record first published: 12 Sep 2012.

To cite this article: Young-Keun Kim, Sang-Eun Cho, Won-Pill Hwang, Min-Hye Seo, Hyun-Woo Park, Mi-Ra Kim & Jin-Kook Lee (2012): Chemically Crosslinked Copolymer Electrolytes Based on Imidazole for Quasi-Solid State Dye-Sensitized Solar Cells, Molecular Crystals and Liquid Crystals, 566:1, 182-192

To link to this article: http://dx.doi.org/10.1080/15421406.2012.701963

Mol. Cryst. Liq. Cryst., Vol. 566: pp. 182–192, 2012
Copyright © Taylor & Francis Group, LLC
ISSN: 1542-1406 print/1563-5287 online
DOI: 10.1080/15421406.2012.701963

Chemically Crosslinked Copolymer Electrolytes Based on Imidazole for Quasi-Solid State Dye-Sensitized Solar Cells

YOUNG-KEUN KIM, SANG-EUN CHO, WON-PILL HWANG,
MIN-HYE SEO, HYUN-WOO PARK, MI-RA KIM,*
AND JIN-KOOK LEE*

Department of Polymer Science & Engineering, Pusan National University
Jangjeon-dong, Kuemjeong-gu, Busan 609-735, Korea

*In this study, gel electrolytes based on poly(1-vinyl imidazole-*co*-elthylene glycol methyl ether acrylate) (P(VIm-*co*-EGMEA)) as backbone polymer and 1,5-diiodopentane ($I(CH_2)_5I$) as crosslinker were used for quasi-solid state dye-sensitized solar cells (QS-DSSCs). Chemically crosslinked gel electrolyte using certain concentration of P(VIm-*co*-EGMEA) and $I(CH_2)_5I$, DSSCs were fabricated and their photovoltaic performances measured by using a Solar Simulator. In order to characterize the electrolytes, resistance of the DSSCs and ionic conductivity of the electrolyte (0.035M of P(VIm-*co*-EGMEA)) was examined by Electrochemical Impedance Spectroscopy (EIS) and the nanopore-filled electrolytes into the nanocrystalline TiO_2 film were investigated by using a Scanning Electron Microscope (SEM).*

Keywords Dye-Sensitized Solar Cells; gel electrolyte; chemically crosslink; Photovoltaic performance

1. Introduction

Dye-sensitized solar cells (DSSCs), considered to be promising photovoltaic devices, were first reported by Grätzel in 1991 [1]. DSSCs have received much attention from many researchers due to their low production cost in comparison with conventional silicon solar cells, simple preparation procedure, and relatively high-energy conversion efficiency [2]. The photovoltaic effect of a DSSC originates from the interface between a redox electrolyte containing iodide and tri-iodide (I^-/I_3^-) ions and a dye-adsorbed nanocrystalline TiO_2 film. The electrolyte provides internal electric conductivity by diffusing within the nanocrystalline TiO_2 film and is an important factor in determining cell performance [3]. Until now, the overall power conversion efficiency of a DSSC based on liquid electrolyte has reached 11.1% under 100 mW/cm^2 (AM 1.5) of irradiation [4]. However, liquid electrolytes have some problems. First, this type of electrolyte contains volatile solvents that cause redox couple mobility, which can lead to leakage and volatilization of the electrolyte. Second, iodine (I_2) is sublimated in air when added to make a redox couple (I^-/I_3^-), and it actually escapes from the cell unless the cell is hermetically sealed. As a result of these

---

*Address correspondence to Mi-Ra Kim, and Jin-Kook Lee, Tel: +82-51-510-3045; Fax: +82-51-513-7720. E-mail: mrkim2@pusan.ac.kr; leejk@pusan.ac.kr problems, the performance of DSSC devices based on liquid electrolytes decays during long-term operation, which limits their practical use. Therefore, in order to replace commonly used liquid electrolytes, solid state and quasi-solid state electrolytes are uesd for the purpose of solidifying electrolytes.

To obtain a solid state or quasi-solid state electrolyte, organic materials, including polymers and oligomers, or inorganic materials can be added [5–9]. Using a p-type semiconductor and organic hole-transport materials are other ways to solidify an electrolyte [10, 11]. Compared with other kinds of charge transport materials, polymers have some advantages, including high ionic conductivity, which is achieved by trapping a liquid electrolyte in polymer cages formed in a matrix, and good contacting and filling properties with the nanocrystalline TiO_2 film and counter electrode [12]. Even though polymers show good contacting properties with the electrode, they are not sufficient for use in DSSCs, which are characterized by high power conversion efficiency due to their high viscosity. Recently, chemically crosslinked gel electrolytes have become an attractive alternative for use in QS-DSSCs. These electrolytes have some advantages. First, the low viscosity of the precursor electrolytes promotes penetration into the nanocrystalline TiO_2 layer. Second, quaterization reactions occur in the presence of the iodide/triiodie redox couple, which solidifies liquid electrolytes *in situ* of the cells. Third, the reaction can be carried out at moderate temperature without any initiators. Accordingly, many researchers are currently using backbone polymers containing pyridine or imidazole. Since the nitrogen atom in pyridine or imidazole contains a lone pair of electrons, it can chemically crosslink with dihalogen derivatives [13].

In this study, P(VIm-*co*-EGMEA) was synthesized as a backbone polymer since homopolymer of Poly(1-vinyl imidazole) (P(VIm)) showed poor solubility in a mixture of EC and PC. Based on the use of P(VIm-*co*-EGMEA) as the gel electrolyte, QS-DSSCs were fabricated and their photovoltaic performances measured by using a Solar Simulator. In order to characterize electrolytes, resistance of the DSSCs and the ionic conductivity of the electrolytes were examined by EIS. The nanopore-filled electrolytes in the nanocrystalline TiO_2 film were investigated by using a SEM.

2. Experimental

2.1. Materials

F-doped SnO_2 glass (FTO glass, 15 Ω/square) as a TCO was purchased from Asahi. TiO_2 paste Ti-Nanoxide HT/SP (particle size: 9 nm) and 1-propyl-3-methylimidazolium iodide (PMII) as an ionic liquid were purchased from Solaronix SA. Iodine (I_2), propylene carbonate (PC), ethylene carbonate (EC), acetonitrile (AN), tetrabutylammonium iodide (TBAI), 1-Vinyl imidazole and ethylene glycol methyl ether acrylate (EGMEA) ($M_W = 13.014$) were purchased from Sigma Aldrich Co., Ltd and used without purification. Hydrogen hezacholroplatinate(IV) solution (H_2PtCl_6) and $I(CH_2)_5I$ ($M_W = 323.94$) were purchased from TCI Co., Ltd. N719 dye (*cis*-diisothiocyanato-bis(2,2'-bipyridyl-4,4'-dicarboxylato) ruthenium(II) bis(tetrabutyl-ammonium)) was purchased from Solchem Co., Ltd.

2.2. Synthesis of P(VIm-co-EGMEA)

P(VIm-*co*-EGMEA) was synthesized as follows. An absolute ethanol solution (20 mL) of 2,2′-azobis(2-methylpropionitrile) (AIBN, 600 mg, 3.65 mmol) was added as an initiator to an absolute ethanol solution (10 mL) of 1-vinyl imidazole (1.9 mL, 21 mmol) and EGMEA (0.45 mL, 3.5 mmol) at a 6:1 molar ratio of monomer using syringe in N_2 Atmosphere. The solution was stirred for 4 h at 80°C. After cooling to room temperature, the solution was poured into ether to initiate precipitation. The resulting white precipitate was filtered and dried at room temperature *in vacuo*. Yield: 2.1 g, 86%. M_n: 4,915. M_w: 5,086. PDI: 1.035. δ_H(500 MHz; DMSO-d_6; Me_4Si) 8.1–6.6 (imidazole ring), 4.1–3.6 (-C(=O)O-($C\underline{H_2}$)$_2$-O-CH_3), 3.1–3.2 (-C(=O)O-(CH_2)$_2$-O-$C\underline{H_3}$), 2.3–0.9 (polymer backbone).

2.3. Preparation of Electrolytes

The reference liquid electrolyte was composed of 0.24 M I_2, 0.49 M TBAI, 0.79 M PMII, and EC/PC (4:1) in AN. Various amounts of P(VIm-*co*-EGMEA) and $I(CH_2)_5I$ were dissolved in the liquid electrolyte in order to form precursor electrolytes. To investigate the dependence of P(VIm-*co*-EGMEA) concentration on quasi-solid state DSSC performance, P(VIm-*co*-EGMEA) was dissolved in increasing amounts of the liquid electrolyte from 0.025 M to 0.045 M. We fixed the molar ratio of P(VIm-*co*-EGMEA) and $I(CH_2)_5I$ at 2:1. Every electrolyte was continuously stirred at room temperature for 24 h in order to obtain a homogeneous solution.

2.4. Fabrication of DSSCs

We prepared the DSSCs, which were sandwich-type composed of nanocrystalline TiO_2 film, ruthenium dye (N719 dye) molecules, electrolytes, and a Pt counter electrode. The electrodes were prepared as previously described [14]. To assemble the QS-DSSCs using the gel electrolytes, each of the precursor electrolytes was casted on the working electrode and dried in a 55°C oven for 10 min to the evaporate solvent. Then, the working electrode and counter electrode were clamped together, after which the intervening space between two electrodes was filled with the precursor electrolyte. The DSSCs were then heated at 55°C for 10 min to obtain the chemically crosslinked gel electrolyte. To assemble the DSSCs using liquid electrolyte, the working electrode and counter electrode, which has two holes for injection of electrolyte, were attached using a 60 μm thick surlyn, after which the space between the two electrodes was filled with the liquid electrolyte. After the injection of electrolyte, the two holes in the counter electrode were sealed using cover glasses in order to avoid evaporation of the electrolyte.

2.5. Measurements

In order to confirm the structure of the synthesized copolymer (P(VIm-*co*-EGMEA)), we measured its ^{1}H-NMR spectra on a FT-NMR Spectrometer (Unity-Inova 500 MHz) using $CDCl_3$ and DMSO-d_6 as the d-solvent, as well as by Fourier Transform Infrared Spectroscopy (FT-IR, Spectrum GX). Molecular weight was measured using High Speed Gel Permeation Chromatography (Waters 515 pump based system).

The photovoltaic performances of DSSCs were measured using a Solar Simulator (150 W simulator, PEC-L11, PECCELL) under a simulated solar light equipped with an ARC Lamp power supply (AM 1.5, 100 mW/cm^2). The solar simulator was calibrated to a Si reference cell that was verified before the measurement. The active area of DSSCs was 0.25 cm^2. The resistance and ionic conductivity of the electrolytes were examined by EIS. The EIS data were measured with an impedance analyzer (Reference 600, GAMRY instruments) in the frequency range of 1–10^6 Hz at room temperature using stainless steel/electrolyte/stainless steel and full cells, and fitted by Z-MAN software (WONATECH) and Echem analyst (GAMRY). The nanopore-filled electrolytes in the nanocrystalline TiO_2 film were investigated by using a SEM (HITACHI S3500N).

3. Results and Discussion

3.1. Characterizations of Copolymers

FT-IR and ^{1}H-NMR spectroscopy were used to analyze the structure of synthesized P(VIm-*co*-EGMEA). In the FT-IR spectrum, absorption peaks appeared at 1653, 1499, and 1413 cm^{-1} indicating –C=N- groups (imidazole ring). Further, an absorption peak appeared at 1280 cm^{-1} indicating a –C-N- group (imidazole ring). Otherwise, absorption peaks of ester and ether groups of EGMEA appeared at 1728 (-C(=O)- of ester group), 1229 (ether group), 1176 (-C-O- of ester group), and 1086 cm^{-1} (ether group). The monomer ratio in P(VIm-*co*-EGMEA) was measured by ^{1}H-NMR spectroscopy. The three hydrogen peaks of the imidazole ring were compared with the three hydrogen peaks of the methyl group of EGMEA. As a result, the ratio of the two peaks was determined to be 3.8:1 based on integration of the peaks.

3.2. Characterization of Gel Electrolyte

P(VIm-*co*-EGMEA) and $I(CH_2)_5I$ were added into $TBAI/I_2/EC/PC$, and the resulting electrolytes were employed for fabrication of DSSCs. The molar ratio of P(VIm-*co*-EGMEA) and $I(CH_2)_5I$ was fixed at 2:1. The chemical cross-linking reaction between P(VIm-*co*-EGMEA) and $I(CH_2)_5I$ is illustrated in Figure 1. The reaction was carried out at 55°C without any initiators, which prevents the introduction of residual impurities in the gel electrolytes. To confirm gel formation before adding the precursor electrolyte into the cell, we tested the chemical cross-linking reaction between P(VIm-*co*-EGMEA) and $I(CH_2)_5I$ at different concentrations in vials. Figure 2 shows images of the precursor electrolyte and gel electrolyte. After heating at 55°C for 10 min, the electrolytes turned into gel by the formation of three-dimensional polymer networks after the chemical cross-linking reaction. Complete gelation was detected in the electrolytes containing over 0.025 M of P(VIm-*co*-EGMEA). The resultant gel electrolytes were homogeneous and transparent. This result suggests that P(VIm-*co*-EGMEA) interacted too much with the liquid electrolyte. Therefore, when the interaction between the gelator (P(VIm-*co*-EGMEA)/$I(CH_2)_5I$) and liquid

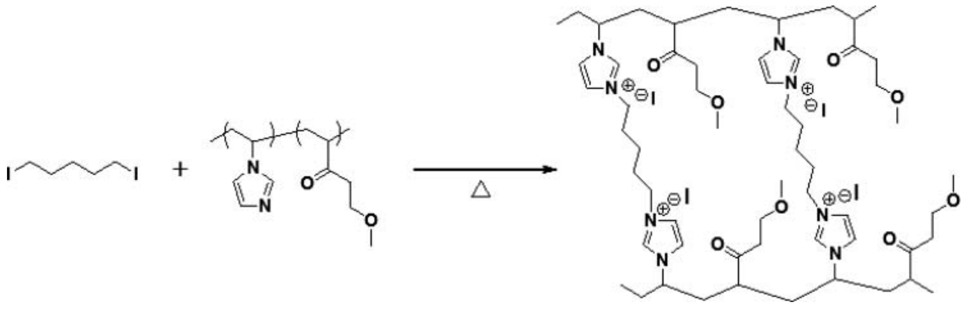

Figure 1. The chemically crosslinking reaction of P((VIm-*co*-EGMEA) and $I(CH_2)_5I$.

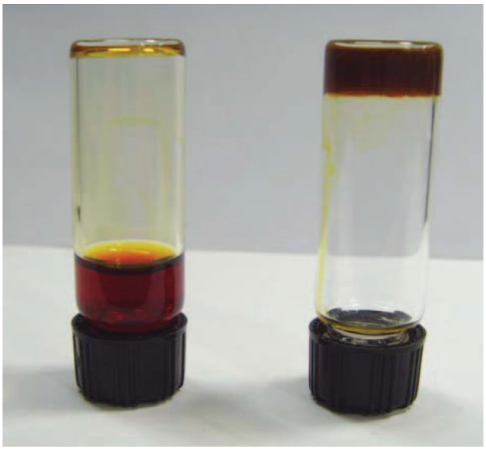

Figure 2. Images of the precursor electrolyte (0.035 M of the copolymer) and the gel electrolyte (after heating).

electrolyte is poor, the gelator reacts by itself and the electrolyte remains as is, resulting in complete two-phase separation [15].

3.3. Short-circuit Photocurrent (J_{sc})

The photovoltaic performances of DSSCs containing different concentrations of P(VIm-*co*-EGMEA) are listed in Table 1. Large differences were found among DSSCs containing liquid electrolyte, precursor electrolyte, and gel electrolyte. Compared with liquid electrolyte, precursor electrolyte showed a decreased J_{sc} value. After adding P(VIm-*co*-EGMEA), the viscosity of the electrolytes increased. The high J_{sc} value of liquid electrolyte can be attributed to the less retarded mobility of the triioide ions as compared to electrolyte containing P(VIm-*co*-EGMEA) in the redox media. The J_{sc} value of the gel electrolytes containing different concentrations of P(VIm-*co*-EGMEA) (0.025 M, 0.030 M, 0.035 M, 0.040 M, and 0.045 M) are listed in Table 1. The J_{sc} value of the DSSCs increased from

Table 1. The Photovoltaic Performances of the DSSCs

Concentration of copolymer	V_{oc} (V)	J_{sc} (mA/cm^2)	Fill Factor	Efficiency (%)
0 M[1]	0.70	11.92	0.56	4.62
0.025 M	0.64	7.11	0.57	2.58
0.030 M	0.66	7.23	0.56	2.67
0.035 M (before heating)[2]	0.75	7.23	0.55	2.97
0.035 M	0.66	8.91	0.60	3.52
0.040 M	0.66	8.14	0.59	3.14
0.045 M	0.63	7.49	0.56	2.67

[1] Liquid electrolyte.

[2] Precursor electrolyte.

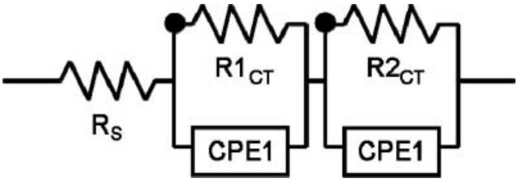

Figure 3. Equivalent circuit of DSSCs. (R_S : series resistace, $R1_{CT}$: charge transfer resistance between Pt counter electrode and electrolyte, CPE1 : constant phase element, $R2_{CT}$: charge transfer resistance between TiO_2 film and electrolyte, CPE2 : constant phase element)

0.025 M to 0.035 M of P(VIm-*co*-EGMEA) and then decreased at higher concentration. The criterion for building a matrix in the electrolyte is liquid electrolyte permeation, which is dependent upon the characteristics of the soaked liquid electrolyte and microcosmic structures of the matrix. The porosity of the matrix increased with increasing concentration of polymer and then slightly decreased [16]. The high porosity of the matrix is good for permeation of the liquid electrolyte into the matrix. Specifically, higher liquid electrolyte permeation in the matrix of the electrolyte increases ion transport in the gel electrolytes [17]. Therefore, the J_{sc} value increased with the addition of 0.035 M P(VIm-*co*-EGMEA) in the electrolyte and decreased upon further addition.

To confirm these results, the interface charge transfer resistances were investigated by using an impedance analyzer. Using EIS measurements, the series resistance (R_S), the charge transfer resistance of the Pt/electrolyte interface ($R1_{CT}$), and the charge transfer resistance of the TiO_2/electrolyte interface ($R2_{CT}$) were measured using the equivalent circuit of the DSSCs shown in Figure 3. The R_S, $R1_{CT}$, and $R2_{CT}$ values of the DSSCs containing various concentrations of gel electrolytes are shown in Table 2. The R_S and $R1_{CT}$ values were not significantly different when using gel electrolytes containing various concentrations of P(VIm-*co*-EGMEA). The $R2_{CT}$ values showed similar behavior as that of J_{sc} value. It can be seen that $R2_{CT}$ decreased from 21.80 Ω to 18.03 Ω as the concentration of P(VIm-*co*-EGMEA) increased from 0.025 M to 0.035 M.

To determine the effect of gelation, we compared the gel electrolyte (0.035 M of P(VIm-*co*-EGMEA)) with the precursor electrolyte (0.035 M of P(VIm-*co*-EGMEA)), and the results are shown in Figure 4. Despite the more viscous nature of the gel electrolyte, the J_{sc} value of the gel electrolyte was higher than that of the precursor electrolyte. After gelation, a three-dimensional network was formed due to the chemical cross-linking reaction between P(VIm-*co*-EGMEA) and $I(CH_2)_5I$. This reaction immobilized the cations and

Table 2. The R_S, $R1_{CT}$ and $R2_{CT}$ Values of the DSSCs using the Gel Electrolytes

Concentration of copolymer	R_S	$R1_{CT}$	$R2_{CT}$
0 M[1]	11.61	6.88	17.87
0.025 M	12.05	6.48	21.80
0.030 M	12.19	6.93	21.33
0.035 M	11.66	6.68	18.03
0.040 M	11.35	6.47	19.92
0.045 M	12.21	6.35	21.47

[1] Liquid electrolyte.

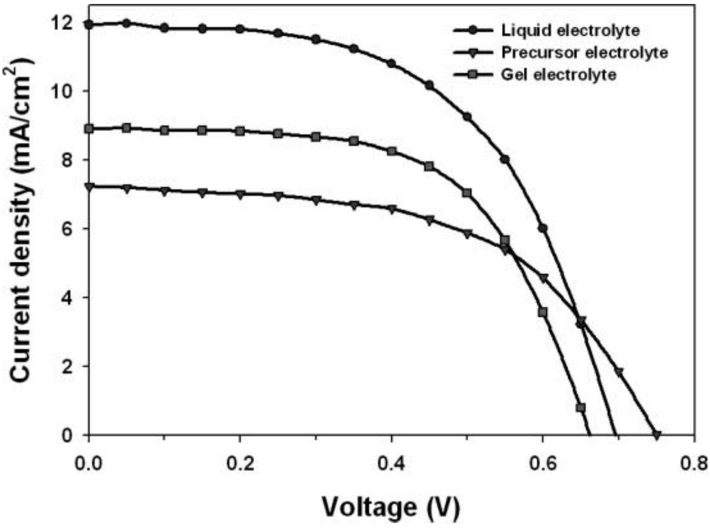

Figure 4. The I-V curve of the DSSCs.

facilitated anionic transport in the gel electrolyte. Consequently, the diffusion of I^- ions was facilitated in the gel electrolyte due to its ionic nature. Therefore, ionic conductivity in the gel electrolyte (1.01×10^{-4} Scm^{-2}) was higher than that in the precursor electrolyte (0.87×10^{-4} Scm^{-2}), and J_{sc} increased from 7.23 to 8.91 mA/cm^2.

3.4. *Open-circuit Voltage (V_{oc})*

Compared with the liquid electrolyte, the precursor electrolyte showed an increased V_{oc} value. This increase in V_{oc} was due to the effect of the imidazole groups of P(VIm-*co*-EGMEA). Additives in the electrolytes such as the pyridine and imidazole derivatives were added to the electrolytes to enhance the V_{oc} value. Adsorption of P(VIm-*co*-EGMEA) to the TiO_2 surface was caused by the interaction between Ti(IV) ion, which is a Lewis acid, and the lone electron pair of the imidazole groups of P(VIm-*co*-EGMEA) [18]. Due to the adsorption of pyridine and imidazole groups on the TiO_2 surface, the recombination of photo-generated electrons from TiO_2 to tri-iodide in the electrolyte was efficiently suppressed. The charge recombination current of the precursor electrolyte was lower than that of the liquid electrolyte. Therefore, the V_{oc} of the precursor electrolyte was higher than that of the liquid electrolyte.

The V_{oc} decreased after gelation, 0.035 M of P(VIm-*co*-EGMEA) since the lone electron pair of P(VIm-*co*-EGMEA) was consumed in the chemical cross-linking reaction. To increase the V_{oc} values of the gel electrolytes, we added tert-butylpiridine (TBP) to the precursor electrolytes. After adding TBP, the chemical cross-linking position decreased due to competition between P(VIm-*co*-EGMEA) and TBP toward $I(CH_2)_5I$. Therefore, the chemical cross-linking reaction was inhibited [19].

3.5. *Fill Factor (FF) and Power Conversion Efficiency (η)*

Compared to liquid electrolyte, the precursor electrolyte showed a slightly decreased FF. Usually, FF of the DSSCs containing polymer gel electrolyte was much lower than that containing liquid electrolyte due to the high viscosity of the polymer gel electrolyte. However, since we used the chemical cross-linking system, a lower concentration of polymer could be used compared to that of the normal polymer gel electrolyte for gelation. Another reason for the lower FF could be the hydrophilic character of P(VIm-*co*-EGMEA), which can easily adsorb to the hydrophilic TiO_2 film surface. As a result of the high interfacial contact between the precursor electrolyte and TiO_2 film, FF was maintained at a similar value after the addition of P(VIm-*co*-EGMEA). The increased FF value following gelation can reasonably be attributed to the increased adsorption of an imidazole group onto the essentially hydrophilic TiO_2 film surface, which was due to the higher hydrophilic character of quaternary salt produced by the chemical cross-linking reaction. However, when the concentration of P(VIm-*co*-EGMEA) was higher than 0.035 M, the FF value decreased with increasing concentration of P(VIm-*co*-EGMEA) due to the increased viscosity of the precursor electrolytes.

After the addition of P(VIm-*co*-EGMEA) to the liquid electrolyte, the η value decreased along with the J_{sc} value upon increasing V_{oc} value. The optimum η value was achieved at 0.035 M of P(VIm-*co*-EGMEA). Upon the increase in FF, an η value of 3.52% with maintenance over 76% was achieved as compared to that of 4.62% for the liquid electrolyte.

3.6. Surface Morphology of Electrolyte-Filled TiO_2 Electrode

The interfacial contact between electrolyte and TiO_2 film is an important factor that determines the photovoltaic performances of DSSCs. To confirm the QS-DSSC of nanopore-filled, chemically crosslinked gel electrolytes into the nanocrystalline TiO_2 film the surface images of the DSSCs were investigated by SEM. The SEM images of the dye-absorbed TiO_2 film impregnated with gel electrolyte containing 0.035 M of P(VIm-*co*-EGMEA) are shown in Figure 5. The gel electrolyte was dropped onto the dye-absorbed TiO_2 film, after which eletcrolyte-filled TiO_2 films were dried for 3 h at 55°C in a dry oven. As shown in Figure 5, P(VIm-*co*-EGMEA) covered the TiO_2 surface. It was observed that the gel electrolytes penetrated into the porous TiO_2 film and were uniformly distributed.

3.7. Long-Term Stability Test

In particular, operational stability is one of the most important factors for a photovoltaic device. This has to a large extent been overcome by good sealing methods and the choice

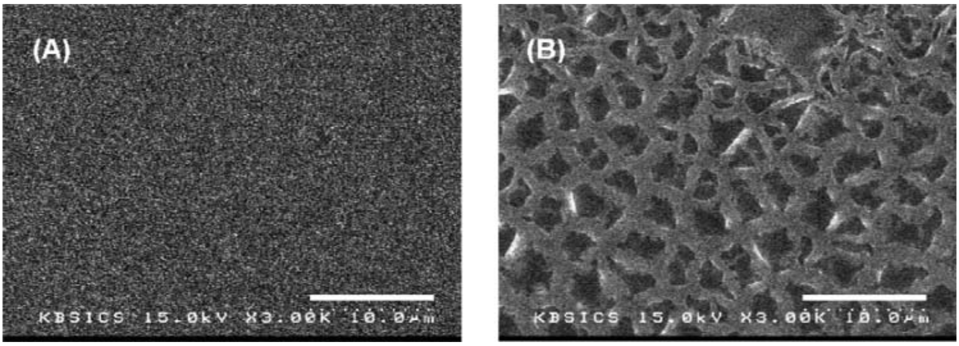

Figure 5. SEM surface images of (A) Bared TiO_2 film and (B) Gel electrolyte filled TiO_2 films on the FTO glass after sintering process.

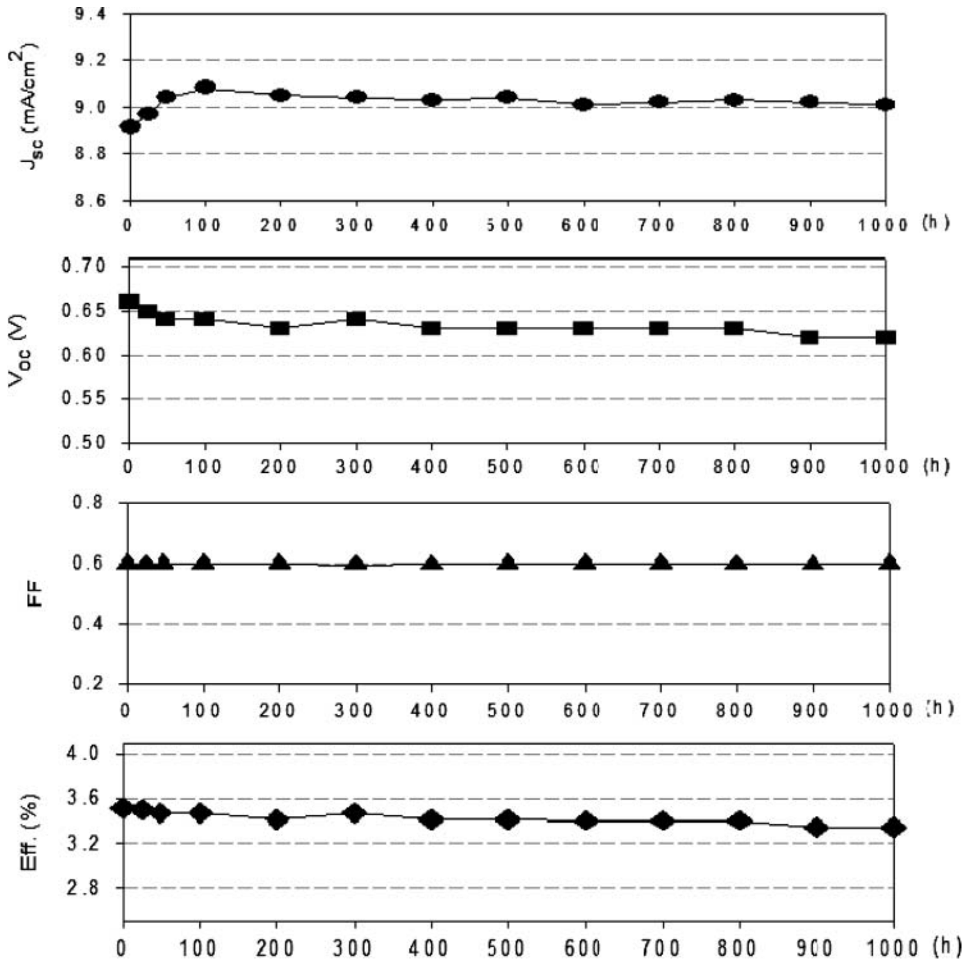

Figure 6. Detailed photovoltaic parameters of a device using chemically cross-linked polymer gel electrolyte for 1,000 h. Current density, J_{sc} (a); Voltage, V_{oc} (b); Fill Factor (c); Efficiency, η (d).

of appropriate chemicals. The DSSC devices were fabricated to long-term stability tests and theirs photovoltaic performance stabilities were measured by using a Solar Simulator. The edges of the devices were sealed with a sealant to protect the corrosion during the long-term stability test, and their long-term stability test was progressed in the dark at 80°C for 1,000 h. The photovoltaic characteristics of the DSSC devices are shown in Figure 6. The initial- / after 1,000 h- photovoltaic performance of the DSSC devices are summarized in Table 3.

These very encouraging results will foster practical applications of DSSC. Figure 6 shows that the J_{sc} increases in performances, while the device maintained over 95% of its initial the V_{oc} and efficiency after 1000 h aging at room temperature in air. In particular, for the FF, no change was observed after 1000 h aging. From this result, it was predicted that the chemically crosslinked gel electrolyte in DSSC devices is being proceeded the chemical reaction during aging on long-term stability tests, and no more increase of J_{sc} showed after the gelation was over.

Table 3. The Initial- / After 1000 h- Photovoltaic Performance of the DSSCs

	V_{oc} (V)		J_{sc} (mA/cm^2)		Fill Factor		Efficiency (%)	
Electrolyte	I[1]	F[2]	I[1]	F[2]	I[1]	F[2]	I[1]	F[2]
Chemically crosslinked polymer	0.66	0.62	8.91	9.01	0.60	0.60	3.52	3.35

[1] Initial value.
[2] Value measured after 1000 h.

4. Conclusion

In this study, gel electrolytes based on P(VIm-*co*-EGMEA) as a backbone polymer and $I(CH_2)_5I$ as a crosslinker were used for the fabrication of QS-DSSCs. P(VIm-*co*-EGMEA) was synthesized and employed to form chemically crosslinked gel electrolyte. Chemical crosslinking reaction occurred between the nitrogen atom of P(VIm-*co*-EGMEA), which has a lone pair electrons, and the diiodide of $I(CH_2)_5I$. Since charge transport in the gel electrolyte was hindered by the P(VIm-*co*-EGMEA) network of the gel electrolyte, the J_{sc} value of the DSSCs containing the gel electrolytes was lower than that containing liquid electrolyte. The FF of the QS-DSSCs increased as a result of a special effect of the imidazole groups from the backbone polymers in the chemical cross-linking reaction. The optimum photovoltaic performance was achieved at 0.035 M of P(VIm-*co*-EGMEA) with $J_{sc} = 8.91$ mA/cm^2, $V_{oc} = 0.66$ V, FF = 0.60, and $\eta = 3.52\%$. The ionic conductivity of the gel electrolyte was 1.01×10^{-4} Scm^{-2}.

Acknowledgement

This research was supported by the Converging Research Center Program through the National Research Foundation of Korea (NRF) funded by the Ministry of Education, Science and Technology (20090082141).

References

[1] O'Regan, B., & Grätzel, M. (1991). *Nature*, *353*, 737.
[2] Ferrere, S., & Gregg, B. A. (2001). *J. Phys. Chem. B*, *105*, 7602.
[3] Wang, Y. (2009). *Sol. Energy Mater. Sol. Cells.*, *93*, 1167.
[4] Kartini, I., Meredith, P., Zhao, X. S., Diniz da Costa, J. C., & Lu, G. Q. (2004). *J. Nanosci. Nanotech.*, *4*, 270.
[5] Kubo, W., Kambe, S., Nkakade, S., Kitamura, T., Hanabusa, K., Wada, Y., & Yanagida, S. (2003). *J. Phys. Chem. B*, *107*, 4374.
[6] Kang, M. S., Ahn, K. S., & Lee, J. W. (2008). *J. Power Sources*, *180*, 896.
[7] Lee, Y. L., Shen, Y. J., & Yang, Y. M. (2008). *Nanotechnology*, *19*, 455201.
[8] Berginc, M., Hočevar, M., Opara Krašovec, U., Hinsch, A., Sastrawan, R., & Topič, M. (2008). *Thin Solid Films*, *516*, 4645.
[9] Li, Z. H., Su, G. Y., Wang, X. Y., & Gao, D. S. (2005). *Solid State Ionics*, *176*, 1903.
[10] Bandara, J., & Weerasinghe, H. (2004). *Sol. Energy Mater. Sol. Cells.*, *81*, 197.
[11] Wang, Y., Yang, K., Kim, S. C., Nagarajan, R., Samuelson, L. A., & Kumar, J. (2006). *Chem. Mater.*, *18*, 4215.

[12] Wu, J., Lan, Z., Wang, D., Hao, S., Lin, J., Wei, Y., Yin, S., & Sato, T. (2006). *J. Photochem. Photobiol. A: Chem.*, *181*, 333.

[13] Li, M. Y., Feng, S. J., Fang, S. B., Xiao, X. R., Li, X. P., Zhou, X. W., & Lin, Y. (2007). *Chinese Science Bulletin*, *52*, 2320.

[14] Jung, K. S., Kim, Y. K., Park, H. W., Won, D. H., Jang, W. Y., Kim, K. H., Seo, M. H., Kim, M. R., & Lee, J. K. (2011). *Mol. Cry. Liq. Cry.*, *538*, 249.

[15] Murai, S., Mikoshiba, S., Sumino, H., & Hayase, S. (2002). *J. Photochem. Photobiol. A: Chem.*, *148*, 33.

[16] Saikia, D., Han, C. C., & Chen-Yang, Y. W., (2008). *J. Power Sources*, *185*, 570.

[17] Lan, Z., Wu, J., Lin, J., Huang, M., Yin, S., & Sato, T. (2007). *Electrochim. Acta.*, *52*, 6673.

[18] Komiya, R., Han, L., Yamanaka, R., Islam, A. and Mitate, T. (2004). *J. Photochem. Photobiol. A: Chem.*, *164*, 123.

[19] Kato, T., Fujimoto, M., Kado, T., Sakaguchi, S., Kosugi, D., Shiratuchi, R., Takashima, W., Kaneto, K., & Hayase, S. (2005). *J. Electrochem. Soc.*, *152*, A1105.